Myosin II-dependent cylindrical protrusions induced by quinine in *Dictyostelium*: antagonizing effects of actin polymerization at the leading edge

Kunito Yoshida and Kei Inouye

Department of Botany, Graduate School of Science, Kyoto University, Sakyo-ku, Kyoto 606-8502, Japan
Author for correspondence (e-mail: yoshida@cosmos.bot.kyoto-u.ac.jp)

Accepted 3 March 2001
Journal of Cell Science 114, 2155-2165 (2001) © The Company of Biologists Ltd

SUMMARY

We found that amoeboid cells of *Dictyostelium* are induced by a millimolar concentration of quinine to form a rapidly elongating, cylindrical protrusion, which often led to sustained locomotion of the cells. Formation of the protrusion was initiated by fusion of a contractile vacuole with the cell membrane. During protrusion extension, a patch of the contractile vacuole membrane stayed undiffused on the leading edge of the protrusion for over 30 seconds. Protrusion formation was not inhibited by high osmolarity of the external medium (at least up to 400 mosM). By contrast, mutant cells lacking myosin II (*mhc*$^{-}$ cells) failed to extend protrusions upon exposure to quinine. When GFP-myosin-expressing cells were exposed to quinine, GFP-myosin was accumulated in the cell periphery forming a layer under the cell membrane, but a newly formed protrusion was initially devoid of a GFP-myosin layer, which gradually formed and extended from the base of the protrusion. F-actin was absent in the leading front of the protrusion during the period of its rapid elongation, and the formation of a layer of F-actin in the front was closely correlated with its slowing-down or retraction. Periodical or continuous detachment of the F-actin layer from the apical membrane of the protrusion, accompanied by a transient increase in the elongation speed at the site of detachment, was observed in some of the protrusions. The detached F-actin layers, which formed a spiral layer of F-actin in the case of continuous detachment, moved in the opposite direction of protrusion elongation. In the presence of both cytochalasin A and quinine, the protrusions formed were not cylindrical but spherical, which swallowed up the entire cellular contents. The estimated bulk flux into the expanding spherical protrusions of such cells was four-times higher than the flux into the elongating cylindrical protrusions of the cells treated with quinine alone. These results indicate that the force responsible for the quinine-induced protrusion is mainly due to contraction of the cell body, which requires normal myosin II functions, while actin polymerization is important in restricting the direction of its expansion. We will discuss the possible significance of tail contraction in cell movement in the multicellular phase of *Dictyostelium* development, where cell locomotion similar to that induced by quinine is often observed without quinine treatment, and in protrusion elongation in general.

Movies available on-line

Key words: Pseudopod, Myosin, Actin polymerization, Contraction, Contractile vacuole

INTRODUCTION

One of the major goals in the study of cell locomotion is to understand the mechanism of the formation and elongation of protrusions in terms of force. There remains controversy over the question as to where the forces are generated during protrusion formation (reviewed by Bray and White, 1988; Harris, 1990; Heath and Holifield, 1991; Condeelis, 1993; Grębecki, 1994; Bretscher, 1996). This is due in part to the complexity of protrusion formation in motile cells, which involves several distinct events, such as disintegration of the cytoskeleton, contraction of the cell cortex, flows of the cytosol towards extending pseudopods, flows of cytoskeletal and membrane components, and reconstruction of the cytoskeleton.

Various hypotheses have been proposed to explain how these processes are coordinated to generate the force responsible for protrusion formation. One of the most classical hypotheses is the 'tail contraction' model (Mast, 1926; Janson and Taylor, 1993; Yanai et al., 1996), which suggests that an increase in the hydrostatic pressure due to contraction of the cortical layer of the cell causes cytoplasmic flow through the membrane region with the smallest resistance to form a pseudopod. Another type of classical hypothesis called the 'frontal contraction' model (Allen, 1961) proposes that sliding forces generated within the pseudopods are responsible for the cytoplasmic flow. Actin polymerization in the leading front of a protrusion (Wang, 1985) is also estimated to produce enough force for the extension of protrusions (Condeelis, 1993; Mogilner and Oster, 1996; Abraham et al., 1999). In some instances, osmotic influx of water accounts for the force required for protrusion extension (Tilney and Inoué, 1985). Membrane components have also been suggested to play important roles in protrusion formation. Bretscher's lipid flow hypothesis states that a continuing cycle of exocytosis at the

leading edge of the cell and endocytosis at its rear end causes a lipid flow on the membrane surface, which not only leads to the uneven distribution of cell surface receptors and capping but also propels the cell forward (Bretscher, 1984).

Although these hypotheses are often regarded as competing ones, it seems more likely that they represent a repertoire of mechanisms for protrusion formation in motile cells. Different mechanisms are probably not mutually exclusive but may coexist and work together within a single cell, and different spatial and temporal combination of these mechanisms, with varied degrees of their manifestation, would result in diverse appearance of pseudopods (such as lamellipodia, filopodia and lobopodia), depending on the cell type and culture condition. Indeed, coexistence of different types of pseudopods, as well as transitions from one type to another, within a cell are common in many kinds of motile cells (Trinkaus, 1973; Harris, 1990; Cunningham, 1995). For analytical studies of force generation in motile cells, it would be necessary, therefore, to resolve the entire process of protrusion formation into elementary processes corresponding to specific mechanisms (or 'modes' of protrusion formation) such as tail contraction and actin polymerization, and to investigate cell movement under conditions where only one 'mode' is predominant.

Amoeboid cells of the cellular slime mould *Dictyostelium* share many features in common with animal cells, and exhibit active cell movement as solitary cells and within multicellular tissues. We found that a millimolar concentration of quinine induces *Dictyostelium* cells to form a rapidly elongating, cylindrical protrusion, which often led to continuous movement of the cells. Analyses under various conditions indicate that the force responsible for quinine-induced lobopodium-like protrusions is generated mainly by contraction of the cell body which requires normal myosin II functions but not actin polymerization itself. In *Dictyostelium*, protrusions of similar appearance are sometimes seen under physiological conditions, most notably with cells dissociated from multicellular tissues undergoing morphogenesis. We suggest that the protrusions observed in the present study represent one of the native modes (tail-contraction mode) of protrusion formation in *Dictyostelium* and possibly in other organisms as well.

MATERIALS AND METHODS

Cells and culture conditions

Cells of *Dictyostelium discoideum* strain Ax2, HS1 (myosin II-null mutant), GFP-myosin-expressing strain (both kindly provided by S. Yumura, Yamaguchi University), and GFP-ABD-expressing strain (a generous gift of D. Knecht, University of Connecticut) were cultivated in axenic medium (Watts and Ashworth, 1970). All the culture and experiments were conducted at ca. 22°C.

Observation with conventional light microscopy

Cells at the exponentially growing phase were allowed to settle on a coverslip or a glass-bottomed plastic culture dish (MarTek Inc., USA). After 10 minutes, the growth medium was replaced with 5 mM MES solution (adjusted to pH 6.2 with Tris) containing various concentrations of quinine, sorbitol and 10 μM cytochalasin A, either singly or in combination as indicated. In standard experiments, cells were observed with an inverted phase-contrast microscope (Nikon TMD) with a 40× objective. To obtain a higher magnification, the coverslip was placed face down on a drop of silicon oil (KF-99, Shin-etsu Chemical co.) on a slideglass. The cells were observed with a phase-contrast upright microscope (Nikon S) with a 100× objective.

To obtain dissociated slug cells, growth phase cells were freed of nutrient by repeated washes in phosphate buffer, and a dense cell suspension was streaked on agar plate containing 20 mM K/Na_2 phosphate buffer pH 7.4. The next day, the streaked part of the agar was cut out and discarded, and slugs migrating on the clean surface of the remaining agar were collected in the same buffer. The slugs were dissociated into single cells by repeated passages through a 25G needle with a 1 ml syringe, and plated in a well made of a coverslip and a square piece of silicon rubber (22×22×2 mm) with a round hole (diameter 15 mm). Excessive buffer was immediately removed so that the remaining buffer formed a thin film of a depth just enough to cover the remaining cells. The hole of the silicon rubber was topped with another coverslip to prevent desiccation, and the cells entrapped within the buffer film were immediately observed with an inverted phase-contrast microscope.

Sequential images were captured at regular intervals with a CCD video camera (Tokyo Denshi, CS8310) connected to a frame grabber board (AG-5, Scion Instruments) mounted on a Macintosh computer. NIH Image 1.62 (developed at the US National Institutes of Health and available on the Internet at http://rsb.info.nih.gov/nih-image/) was used for the control of image capturing (video-rate averaging of 3-8 frames when necessary), image processing and data analysis.

To measure the elongation velocity of a protrusion, an image stack was made of a cell forming a protrusion and an image profile was created using the 'Reslice' function of NIH Image in the direction of the protrusion extension. To estimate the bulk flux into the protrusion, the velocity of the protrusion was multiplied by the cross-section of the protrusion assuming it to be a cylinder of a fixed diameter. To estimate the bulk flux into the spherical bleb formed in the presence of cytochalasin A, the volume of the bleb was calculated from its diameter assuming it to be a sphere. To measure the maximal travelling distance of the inner solid material pushed out of the broken cells, the medium was replaced with 2 mM quinine/2.5 mM MES solution containing 1% methyl cellulose, and sequential images were captured.

Observation of living cells with a confocal laser-scanning microscope

Cells were stained with 1 μg/ml RH 795 in 5 mM MES for 10-20 minutes, and an excess of the same buffer containing 2 mM quinine without the dye was added. By this time, the fluorescence was predominantly localized on the contractile vacuole (John Heuser, personal communication; see http://www.heuserlab.wustl.edu/). Cells were observed with a confocal microscope (Zeiss LSM410) with excitation wavelength at 495 nm and a cut-off wavelength at 515 nm or 505-550 nm with a 63× Neofluar objective (NA 1.4). GFP-myosin-expressing cells and GFP-ABD cells were observed using the same conditions. In many experiments, fluorescence and differential interference contrast (Nomarski) images were simultaneously recorded at regular intervals.

Immunofluorescence

Cells were fixed as described previously (Neuhaus et al., 1998) without ethane-freezing. Briefly, a coverslip carrying the cells was dipped into methanol at –85°C, then the temperature was slowly raised to –35°C over a period of 30 minutes, and the coverslip transferred to PBS at room temperature (temperature lower than 15°C resulted in unsatisfactory fixation of extended protrusions). After washing with PBS three times, the coverslip was incubated with an antibody against the 100 kDa subunit of *Dictyostelium* V-ATPase (N2 antibody; Fok et al., 1993) diluted 1:50 in PBS or an antibody against calmodulin (2D1 antibody) diluted 1:400. After three washes in PBS, the specimens were incubated with a rhodamine-conjugated affinity purified anti-mouse IgG diluted 1:200.

For phalloidin staining, cells that had been incubated in buffer

containing 100 mM sorbitol with or without 1 mM quinine (and 10 μM cytochalasin A) for 1 minute were fixed in 1% glutaraldehyde in 20 mM Na/K phosphate buffer, pH 6.5 for 30 minutes, permeabilized in a 1:2 diluted fixative solution containing 0.2% Triton X-100, and the autofluorescence was quenched in PBS containing 1 mg/ml $NaBH_4$ and 100 mM glycine (Sesaki and Ogihara, 1997; Ginger, 1998). After washing in PBS and incubation in PBS containing 1% BSA, the cells were stained with 1 unit Alexa 568-phalloidin in 50 μl PBS containing 1% BSA for 30 minutes, washed in PBS, and observed with the confocal microscope (excitation wavelength, 543 nm; cut-off wavelength, 590 nm).

Particle tracking

Concanavalin A (ConA) was covalently linked to carboxylate-modified microspheres (FluoSpheres, 0.5 μm, red fluorescence) using a water soluble carbodiimide, 1-ethyl-3-(3-dimethylaminopropyl) carbodiimide (EDAC), according to the manufacturer's instructions (Jay and Elson, 1992). The cells were allowed to settle on a coverslip and incubated in 10 mM MES (pH 6.2) containing ConA-linked fluorescent beads for 5 minutes. After an extensive wash in a large volume of the same buffer to remove unattached beads, the cells were immersed in buffer containing 2 mM quinine, and placed under silicon oil layer (see above). Confocal observation was conducted with the maximal pinhole size.

Materials

The N2 mAb was a generous gift of A. Fok of Hawaii University. Quinine hydrochloride, concanavalin A, cytochalasin A, and the anti-calmodulin antibody (2D1) were purchased from Sigma, RH795, FluoSpheres, EDAC and Alexa-phalloidin were from Molecular Probes, and the anti-mouse IgG was from Chemicon. Silicon oil (KF-99) was a generous gift of Shin-etsu Chemicals.

RESULTS

Morphology and dynamics of quinine-induced protrusions

Vegetative cells of *Dictyostelium* placed on a solid substratum move about by extending numerous filopodia and lamellipodia. When exposed to a millimolar concentration of quinine, they retracted most of the pseudopods to become rounder within a minute, and large translucent vacuoles developed in many cells. These vacuoles were identified as contractile vacuoles because: (1) they showed contraction; (2) they possessed the contractile vacuole markers V-ATPase and calmodulin (see Fig. 3C,D insets) (Zhu and Clarke, 1992; Fok et al., 1993; Heuser et al., 1993; Nolta et al., 1993); and (3) they did not take up a pinocytosis marker fluorescein-dextran (data not shown). The frequency of detectable contraction was significantly lower (0.1±0.15 contractions/cell/minute, n=19 cells with 1 mM quinine, compared with 2.6±1.5 contractions/cell/minute, n=13 cells without quinine), and the maximum sizes of the vacuoles larger, than without quinine. When contraction occurred, however, it was often followed by the formation of a cylindrical protrusion with a round head (Fig. 1B-D). That the protrusions were not flat but cylindrical was confirmed by changing the focus of the microscopes (Nomarski and confocal) and by SEM observations (Fig. 1C). Observation of such cells with a phase-contrast microscope indicated the lack of prominent structures in the apical region of the protrusions (Fig. 1D). Typically the speed of protrusion extension was about 0.7 μm/second, slightly larger than the speed of pseudopod extension in *Dictyostelium* cells (Schindl et al., 1995). The diameter of protrusions ranged from a small fraction of the cell diameter to almost as wide as the cell itself, but in many cases such protrusions elongated until they took up a considerable fraction

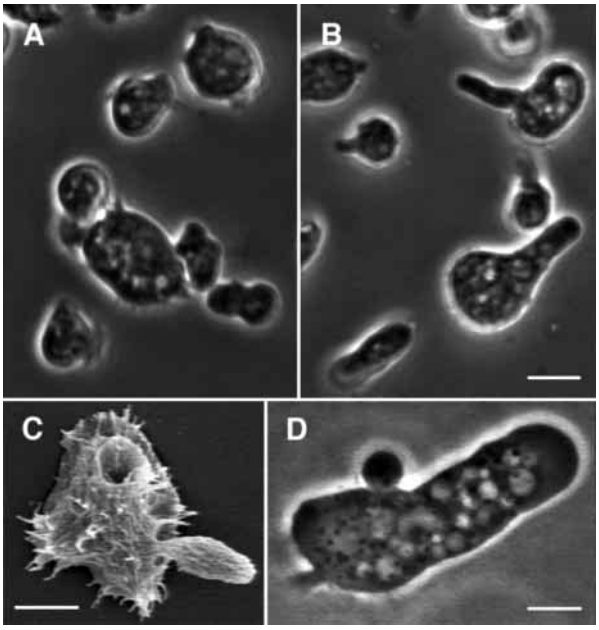

Fig. 1. Phase-contrast images of Ax2 cells 1 minute after exchange of the medium to buffer with (B) or without (A) 2 mM quinine. Also shown are scanning electronmicroscopic (C) and high-magnification phase contrast (D) images of Ax2 cells extending protrusions in response to 2 mM quinine. Bars, 10 μm (A,B); 5 μm (C,D).

Fig. 2. Sequential fluorescence images of an Ax2 cell with an extending protrusion induced by quinine. Cells had been stained with RH-795 10 minutes before quinine application. Time=0, 3.1, 6.2, 9.2, 15.4, 21.5, 27.7, 40.0 and 52.3 seconds from left to right. The estimated area of the apical membrane region with the fluorescence intensity higher than that of the original cell membrane was almost constant throughout the period of elongation. For this calculation, it was assumed that the protrusion is in the shape of a hemisphere attached to a cylinder and that the sections are on the horizontal median plane of the protrusion. In the presence of quinine, the difference in the fluorescence intensity between the contractile vacuole membrane and plasma membrane was usually not as large as without quinine, partly because the contractile vacuole membrane is integrated in the plasma membrane upon its expulsion, as shown here and Fig. 6C. Bar, 10 μm. Movies of this and other sequential images are available at http://www.biologists.com/JCS/movies/jcs1984.html).

of the cell volume. Some cells went further and actually translocated by continuously extending the protrusion while retracting the original cell body, suggesting that the mechanism of elongation of quinine-induced protrusions have some features common to the mechanism of cell movement.

The occurrence of protrusion formation peaked at 1-3 minutes after exposure to quinine. Cells eventually burst (mostly within 30 minutes) in the continuous presence of quinine under low salt conditions (5 mM MES-Tris) even with 200 mM sorbitol. However, cells survived for days with 2 mM quinine if the buffer was supplemented with 20 mM KCl, 1 mM $CaCl_2$, 1 mM $MgCl_2$ or 0.1 mM spermine (in which cases normal aggregation occurred), or if cells were grown in growth medium (in which case cells proliferated).

Membrane markers

Fig. 2 shows sequential photographs of a cell that had been stained with a fluorescence dye RH-795, which has high affinity to the contractile vacuole membranes. The fluorescence on the large vacuole seen in the first frame appeared to translocate to the cell membrane in the next frame at the position where the contractile vacuole had disappeared. It can be seen that the patch of fluorescence stayed on the leading edge of the protrusion without much dispersal over the period of more than 30 seconds of cell locomotion. Immunofluorescence detection of V-ATPase and calmodulin around the tip of the protrusion also indicates its origin to be the contractile vacuole membrane (Fig. 3). These protein markers remained undiffused for at least 5 minutes.

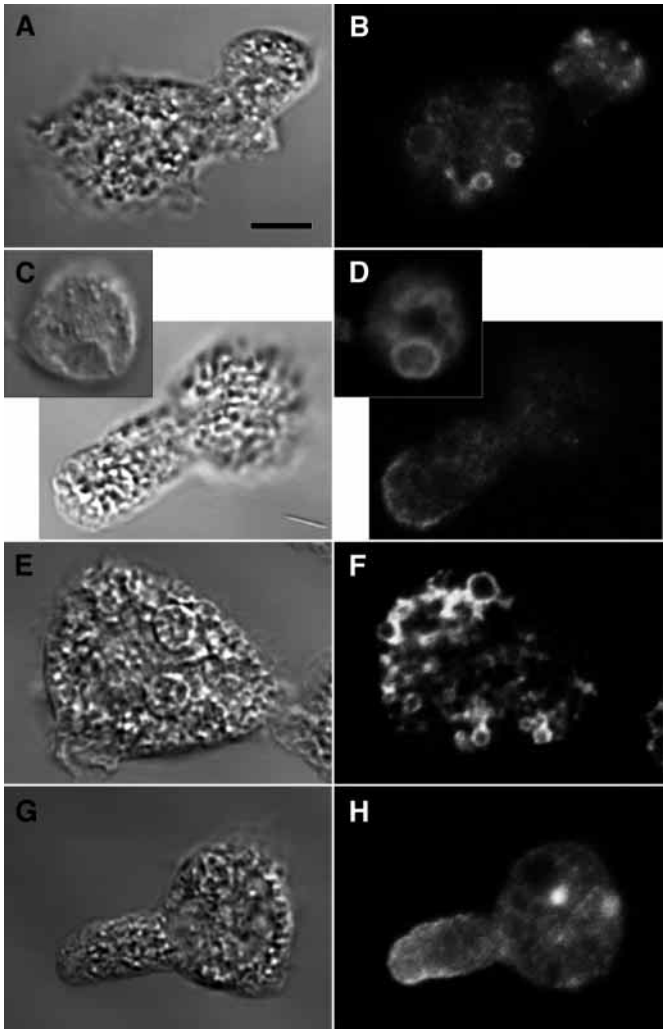

Fig. 3. Nomarski contrast (left column) and immunofluorescence (right column) images of control cells (A,B,E,F) and quinine-treated cells (C,D,G,H) stained with an antibody against the 100 kDa subunit of V-ATPase (A,B,C,D) or an anti-calmodulin antibody (E,F,G,H). Cells were fixed after a 5 minute incubation with 2 mM quinine. Insets in C and D show an enlarged contractile vacuole in a quinine-treated cell. Bar, 5 μm.

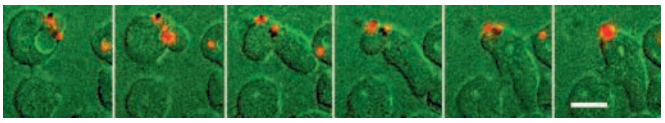

Fig. 4. Sequential images showing concanavalin A-tagged fluorescent beads attached to the cell surface during elongation of protrusion. Fluorescence is shown in red and Nomarski images in green. Intervals between successive frames are 19.4 seconds. Bar, 10 μm.

By contrast, concanavalin A-tagged fluorescent beads attached on the cell surface did not move along with the advancing protrusion but remained stationary relative to the substratum until eventually converged into the rear end of the cell (Fig. 4).

Effects of osmolarity

Fig. 5 shows the velocity of protrusion extension at various concentrations of sorbitol in the presence of quinine. The length of the protrusion also decreased as the sorbitol concentration increased, whereas the diameter of the protrusion remained unchanged, being approximately 5 μm (data not shown). Extrapolation of the fitted line in Fig. 5 indicates that protrusion extension would stop only at 650 mosM, which is much higher than the osmolarity of the cytosol (100-200 mosM; Steck et al., 1997). This implies that the protrusive force cannot be attributed to the passive influx of water downhill the osmotic pressure gradient.

Involvement of myosin II

Cells of a strain lacking myosin II (*mhc*$^-$ cells; Manstein et al., 1989) did not extend protrusions in buffer containing quinine (Fig. 6A,B). Vital staining with RH-795 showed that

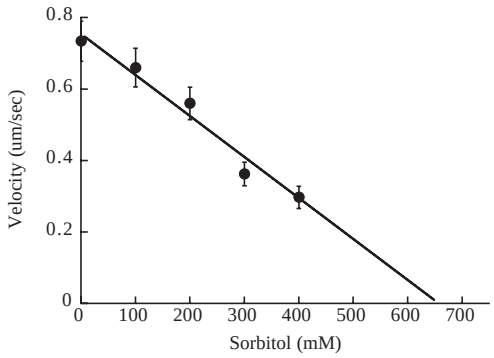

Fig. 5. Dependence of the rate of protrusion elongation on the sorbitol concentration in buffer. Vertical bars indicate means±s.e.m. (n=31, 26, 26, 22, 19, from left to right, respectively).

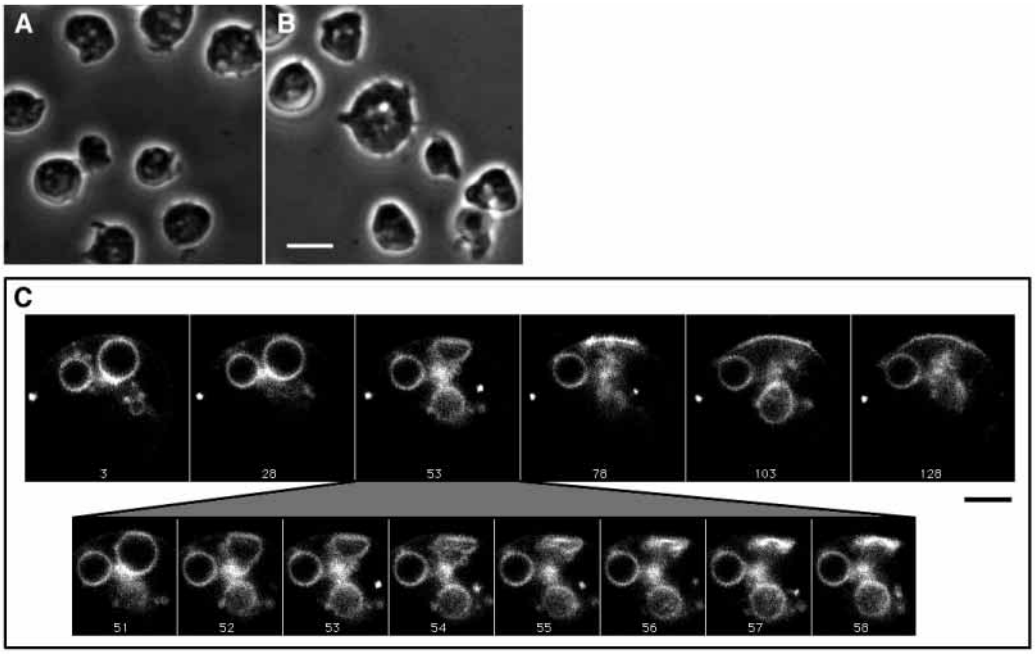

Fig. 6. (A, B) Phase-contrast images of *mhc*⁻ cells 1 minute after exchange of the medium to buffer without (A) or with (B) 2 mM quinine. Bar, 10 μm. (C) Sequential fluorescence images of an *mhc*⁻ cell showing expulsion of a contractile vacuole. The cell had been stained with RH-795 10 minutes before quinine application. A patch of fluorescence stayed on the cell membrane at the site of expulsion of one of the contractile vacuoles. Intervals between successive frames are 13.7 seconds in the upper panel. The intervals in the lower panel are 0.55 seconds to show the moment of discharge at shorter time intervals. Bar, 5 μm.

expulsion of contractile vacuoles did occur, but it did not accompany any noticeable protrusions (Fig. 6C). Cells eventually burst under low ionic conditions as with the case of Ax2 cells. Observation of cells expressing GFP-tagged myosin II (Moores et al., 1996) showed that myosin II molecules accumulated in the peripheral regions of the cells in the presence of quinine (Fig. 7). When a new protrusion appeared, it was initially devoid of myosin II-enriched cortex. When the protrusion stopped elongating (Fig. 7A) or elongated over a substantial distance (usually more than half the length of the entire cell, Fig. 7B), a layer of GFP-myosin started to form on the periphery of the protrusion, progressively from its base towards the tip. The speed of extension of this fluorescent layer towards the distal end of the protrusion (0.12±0.011 μm/second, n=11) was much lower than the typical speed of protrusion elongation. As the entire protrusion became lined with the fluorescent layer, the demarcation between the protrusion and the cell body gradually became less clear and the protrusion began to retract, while in some instances the base of the protrusion became constricted. In the latter case, GFP-myosin accumulated in the constricted region and retraction of the protrusion was usually delayed (not shown).

These observations suggest that myosin-based tail contraction is the source of the protrusive force. This possibility gained further support from the following observations. As mentioned earlier, cells eventually burst in the continuous presence of quinine under low ionic conditions, in which case solid cellular materials are pushed out of the cells en masse, usually protruding in one direction in buffer made viscous with methyl cellulose. It was found that the maximal distance over which the mass of solid inner materials travelled was significantly smaller in myosin-null cells compared with Ax2 cells (Fig. 8).

Actin polymerization

The distribution of F-actin was investigated in cells that had been induced to form protrusions. Phalloidin staining of Ax2 cells that had been bathed in buffer containing quinine for 1 minute showed that the cell body was lined with a thick cortical layer of F-actin, whereas the cortical actin layer in the protrusion was thinner towards its distal end where phalloidin staining was barely visible (Fig. 9C,D). The absence of an F-actin layer in the tip region was confirmed by observation of serial optical sections (Fig. 9E,F). In some cells, thin arc-shaped fluorescence extending from both sides of the protrusion towards its axis were noted in the distal region of their longitudinal section (Fig. 9D). Three-dimensional reconstruction revealed that these fluorescent bands form a continuous spiral at least in some cases (Fig. 9F, insets).

To investigate the changes in F-actin distribution during the

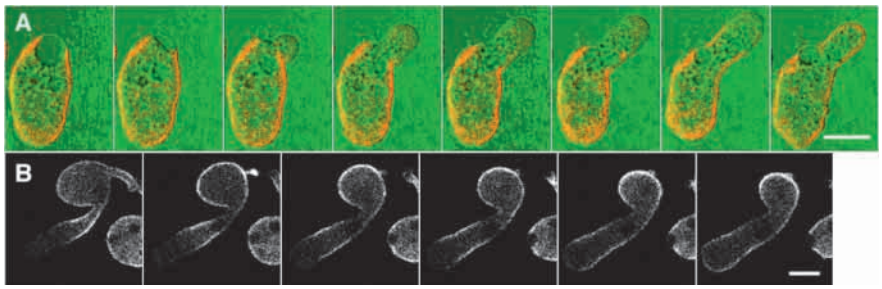

Fig. 7. Changes in the distribution of GFP-myosin II during the formation, elongation and retraction of protrusions in the presence of quinine. (A) Fluorescence is shown in red and Nomarski images in green. Time=0, 5.0, 10.0, 15.0, 20.1, 25.1, 70.9, 142.5 seconds. (B) A cell with a retracting protrusion and a large protrusion that is about to stop extending. The small protrusion is entirely covered with a layer of GFP-myosin, whereas the large protrusion has a constriction at its base, from which a band of GFP-myosin II extends towards the tip. Intervals between successive frames are 47.7 seconds. Bars, 10 μm.

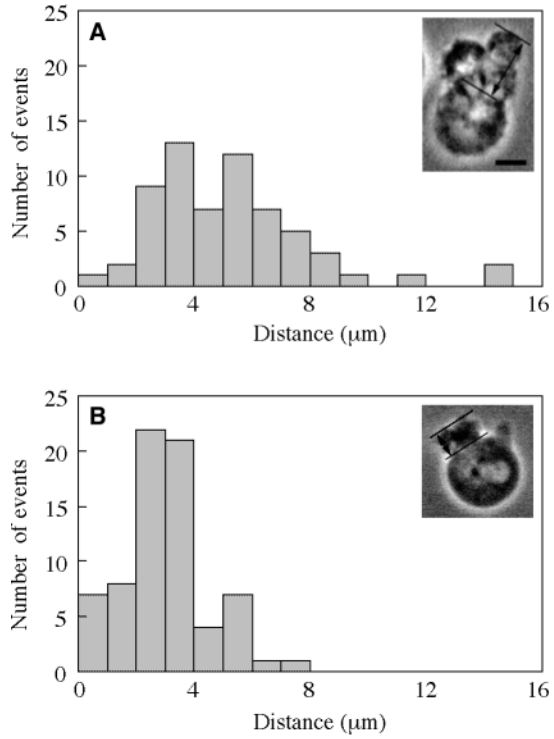

Fig. 8. The distribution of the distance over which the mass of solid cellular materials protruded from lysed cells in the presence of quinine. The buffer contained 1% methyl cellulose to increase the viscosity. The distance between the tip and the base of the protruded solid materials was measured (indicated with the arrows in the insets). (A) Ax2 cells; (B), *mhc*$^{-}$ cells. Bar, 5 μm. Mean±s.e.m. is 5.8±0.4 μm, *n*=62 (A), 3.4±0.2 μm, *n*=70 (B), with the difference being significant (*P*<0.001).

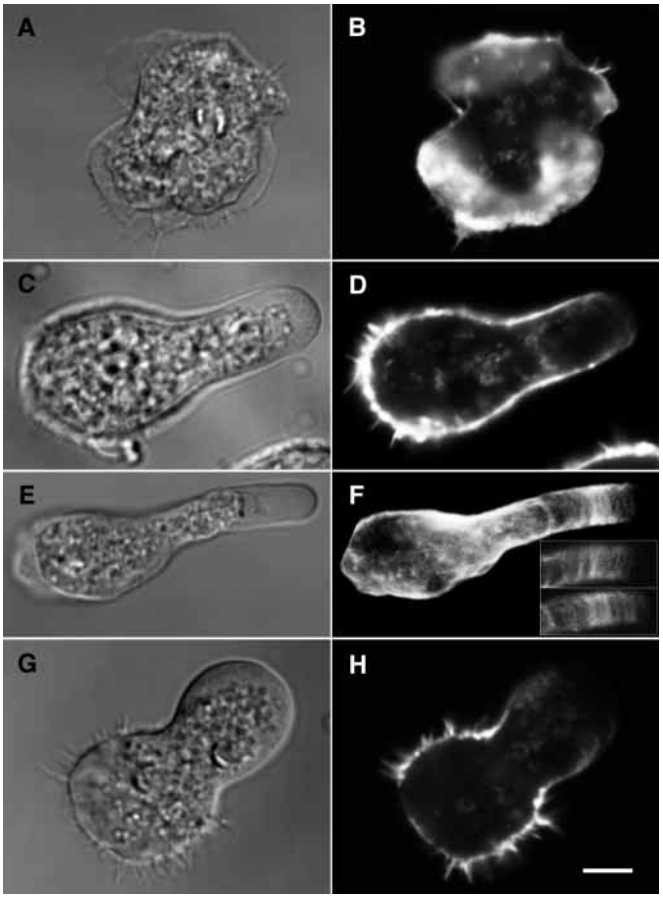

Fig. 9. Nomarski (left) and fluorescence (right) images of cells stained with fluorescent-phalloidin. (A,B) control, (C,D,E,F) quinine, (G,H) quinine and cytochalasin A. The image shown in F is a projection of 30 confocal sections at 0.4 μm intervals covering the entire depth of the cell. Insets in F show the sections on the distal and proximal sides of the protrusion to show that the stripes seen near the tip of the protrusion in F make up a spiral. Bar, 5 μm.

course of protrusion formation, cells expressing the GFP-tagged actin-binding domain of the actin-binding protein ABP-120 (GFP-ABD) were exposed to quinine and induced to form protrusions. GFP-ABD has been shown to specifically and reversibly bind to F-actin in living cells (Pang et al., 1998). The sequential images in Fig. 10A show an example in which a single cell successively formed three protrusions. It can be seen that the apical membrane of the protrusion shows hardly any GFP fluorescence during the period of elongation, whereas it is lined with a clear fluorescent layer during retraction. In cells undergoing sustained locomotion, intense GFP fluorescence was invariably observed in the posterior of the cell (Fig. 10B).

In some cells, arc-shaped lines of GFP-ABD fluorescence were observed to propagate, often repeatedly, from the front end of the protrusions backwards. These fluorescent arcs probably correspond to the F-actin layers observed by phalloidin staining. Three-dimensional reconstruction of cells showing fluorescent waves indicated that these arcs were actually sheets of fluorescence, which in some cases form a continuous spiral (data not shown). Such propagating waves were rarely observable in rapidly elongating protrusions soon after formation (c.f. Fig. 10B) but fairly common in cells that had been bathed in the quinine solution for an extended period. In cells showing clear fluorescent waves, the extension velocity of the apical membrane of the protrusion was not uniform, with intermittent periods of slowing down followed by quick restoration to the maximum speed, and this restoration of speed of the leading front of the protrusion coincided with the detachment of fluorescent arcs from the frontal membrane. This can be visualized by time-space representations of image slices of movies (Fig. 11C,D). Slowing-down of pseudopod expansion by the formation of a cortical layer and restoration to the original speed upon its detachment from the membrane have been described in detail with *Amoeba* and *Chaos* (Grębecki, 1990).

These results strongly suggest that actin accumulates on the inner surface of the extending protrusion to form a thin layer that acts as a mechanical resistance to protrusion extension. To confirm this possibility, we examined the effects of cytochalasin A, which inhibits actin polymerization (Jay and Elson, 1992), on the dynamics of quinine-induced protrusion formation. When the medium was changed to buffer containing both quinine (2 mM) and cytochalasin A (10 μM), cells formed spherical blebs, rather than cylindrical protrusions, with a similar time-course. Discharge of a contractile vacuole preceded the bleb formation, indicating that these spherical blebs and cylindrical protrusions are of the same nature. Fig. 11 shows an example in which a GFP-

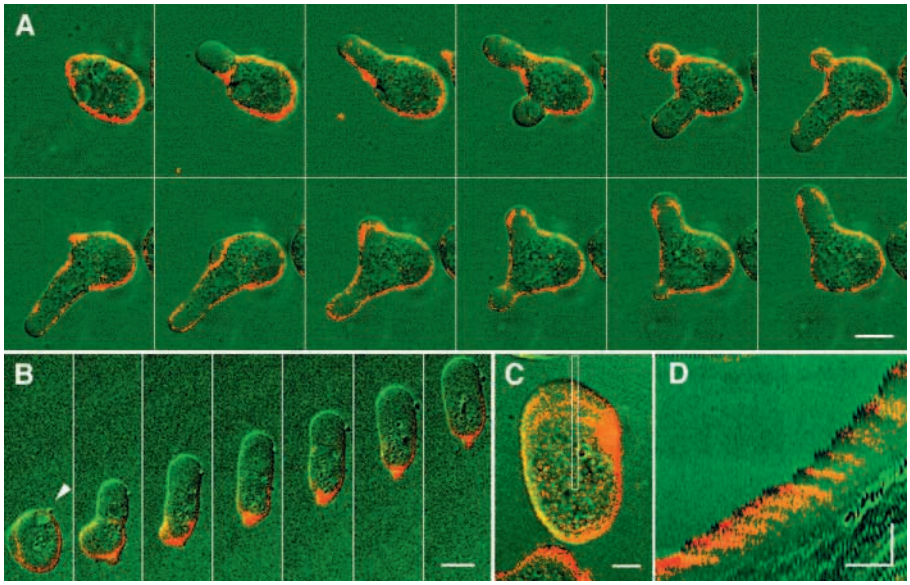

Fig. 10. Sequential images of GFP-ABD cells exposed to quinine (A,B) and fluctuation of the velocity of protrusion elongation accompanying detachment of GFP-ABD layers from the apical membrane of the protrusion (C,D). Fluorescence is shown in red and Nomarski in green. (A) A cell showing successive extension and retraction of protrusions. (B) A cell in locomotion by continuous elongation of a large protrusion. Intervals between successive frames are 10 seconds in A and B. The correlation between the protrusion and a contractile vacuole can be seen in B and for the first two protrusions in A, whereas no contractile vacuole is visible that would have triggered the third protrusion in A. This may be because either it is out of focus or the protrusion was formed independently of a contractile vacuole. In B, a particle (arrowhead) that was accidentally attached or located very close to the cell surface can be seen to move along with the elongating protrusion, which may be indicative of the presence of membrane components that flow forwards. Coexistence of membrane components showing rearward (c.f. Fig. 3) and forward movements have been demonstrated in amoebae and mammalian cells (Grębecki, 1986; Sheetz et al., 1989). Bars, 10 μm. (C,D) Confocal images of another GFP-ABD-expressing cell were taken at intervals of 0.89 seconds, and the images within the thin window (width 1 μm, shown by rectangle in D) on successive frames are arranged from left to right to illustrate the progression of the leading front of the protrusion, the accumulation and rearward propagation of the fluorescence, and their temporal relationship (D). For clarity, D has been expanded twofold in the vertical direction. Horizontal bar in C and vertical bar in D, 5 μm; horizontal bar in D, 10 seconds.

myosin-expressing cell is forming a round bleb in buffer containing quinine and cytochalasin A. It can be seen that the bleb continued growing, while the original cell body with a thick cortical layer of GFP-myosin contracted, to the point where the entire content of the cell body was transferred into the newly formed spherical bleb. Such complete transfer of the cellular content into the bleb was consistently observed. We estimated the bulk flux of cytosol from the original cell body to the bleb, and compared it with the flux in cylindrical protrusions. To do this, the bleb was assumed to be a true sphere, the protrusion to be a cylinder with a uniform diameter, and the flux to be constant. The bulk flux was about four times higher in the spherical blebs than in the cylindrical protrusions (60.7±7.2 μm^3/second (n=36) versus 14.0±1.3 μm^3/second (n=76)), indicating that the formation of actin filaments antagonizes the extension of protrusions rather than causing it. As shown in Fig. 9H, actin filaments were indeed scarce along the membrane of spherical blebs induced by the combination of quinine and cytochalasin A, compared with the lateral membrane of protrusions induced by quinine alone. It should be noted that GFP-myosin in spherical blebs, in contrast to that in elongated protrusions (induced by quinine alone), was not recruited to the submembranous cortex of the newly formed bleb (Fig. 11).

Bleb formation was also observed with cytochalasin A alone, but in this case formation of a bleb is a much slower process, requiring 1 minute at the minimum for its first appearance, and the bleb did not normally engulf the entire cellular content (data not shown).

Bleb formation without drug treatment

Lobopodium-like protrusions are not peculiar to cells treated with quinine or cytochalasin A but also quite common in *Dictyostelium* cells without any drug treatment, as in many other types of cells (reviewed by Taylor and Condeelis, 1979; Harris, 1990). When growth phase cells of *Dictyostelium* are brought from an ice-cold suspension onto glass at 22°C, a small fraction of the cells quickly extend a cylindrical protrusion very similar to those induced by quinine treatment. Such protrusions are, however, much more common in cells at the multicellular stage of development. Fig. 12 shows a cell mechanically dissociated from migrating slugs and placed in a thin film of buffer solution. It can be seen that the cell moves by rapidly extending a large cylindrical protrusion in a manner similar to the quinine-treated cells. Such protrusions lack any detectable F-actin in their front end (Fig. 12B) as in quinine-induced protrusions.

DISCUSSION

The quinine-induced protrusion formation has many advantages as a simple model system to study the mechanism of the formation and extension of protrusions in motile cells:

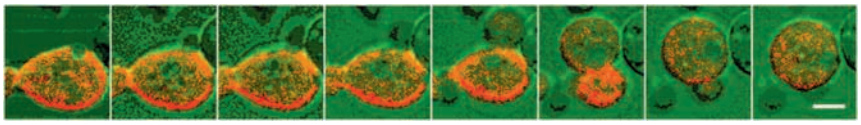

Fig. 11. Bleb formation in the presence of quinine and cytochalasin A. Fluorescence of GFP-myosin II is shown in red, Nomarski in green. Bar, 5 μm. Intervals between successive frames are 2.7 seconds.

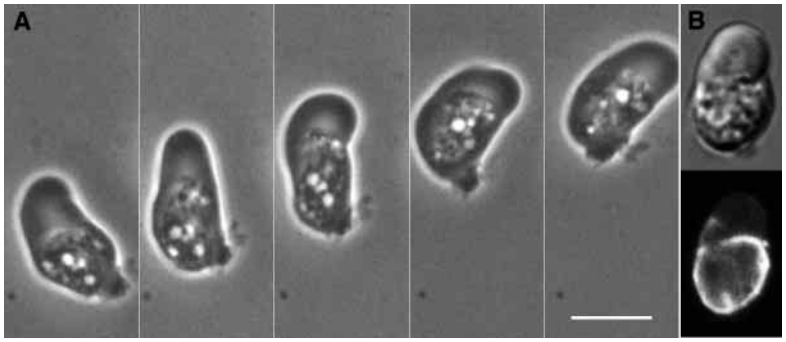

Fig. 12. (A) Sequential phase-contrast images of a mechanically-dissociated slug cell that shows continual locomotion in a thin layer of phosphate buffer without quinine. Intervals between successive frames are 8.0 seconds. The mean velocity of the cell front is 0.76 μm/second. (B) Nomarski (top) and fluorescence (bottom) images of a dissociated slug cell with an elongated protrusion stained with fluorescent phalloidin. Bar, 10 μm.

(1) The protrusion is large and easily observable; (2) the protrusion is unipolar and its polarity can be clearly identified; (3) the boundary between the protrusion and the remaining part of the cell is clear; (4) its formation is rapid and can be easily induced without using chemotactic stimuli which would concurrently elicit various chemotaxis-specific events in the cell; (5) fusion of a contractile vacuole initiates the whole process, which serves as an identifier of the kind of the protrusion under study.

Although the mechanism for the induction of protrusion formation by quinine remains to be clarified, the effect of quinine is most likely an indirect one. Quinine is a general K^+ channel blocker, and we previously showed that it blocks the voltage-dependent K^+ channel found in a fraction enriched in contractile vacuole membranes of *Dictyostelium* (Yoshida et al., 1997). As shown in the present study, the activity of contractile vacuoles in vivo was also affected by quinine under low ionic conditions. However, the toxic effect as well as the induction of protrusion formation was abolished by addition of the growth medium or salts to the buffer, in which cases cells can grow or develop depending on what was added (see also Van Duijn et al., 1989), suggesting both effects to be mainly ionic. Presumably, the altered ionic transport would impair the osmotic regulation of the cell, causing a rise of its internal pressure, and would lead to herniation of contractile vacuoles and eventual bursting of the cell.

Whatever the mechanism, the cylindrical protrusion induced by quinine has some features common to naturally observed pseudopods. First, its elongation can lead to locomotion of the cell. Second, conA beads attached to the surface of the protrusion stayed in the same place with respect to the substratum during its elongation and were converged at the rear edge if the cell continued locomotion as in many types of pseudopods including ones observed in *Dictyostelium* cells (Jay and Elson, 1992). Also, the speed of extension was in the same order as the maximal elongation speed of naturally observed pseudopods (Schindl et al., 1995). By contrast, it differs from pseudopods observed in many kinds of motile cells spreading on solid substrata in that it is cylindrical rather than flat and has smooth and round ends, where F-actin is undetectable or forms only a very thin layer. Protrusion formation of this kind, usually referred to as blebs or lobopodia, is often incorrectly considered as artefacts seen only in unhealthy cells, but in fact they are common under normal conditions (Harris, 1990; Grębecki, 1994; Cunningham, 1995; Keller and Bebie, 1996). For instance, blebbing is a regular feature of some cells during spreading (Erickson and Trinkaus, 1976), mitosis (Boss, 1955), and development (Trinkaus, 1973), and it is also common in *Dictyostelium* cells at the multicellular stage, as shown in this study.

Immunofluorescence and vital staining data demonstrate the insertion of expulsed contractile vacuole membranes into the leading edge of the protrusions. Although protrusion formation initiated by expulsion of a contractile vacuole may be unusual, only shown so far to occur in a mutant of *Dictyostelium discoideum* lacking drainin (a protein involved in contractile vacuole discharge; Becker et al., 1999), formation of a protrusion by an exocytic event is very common. There is evidence that the leading edge of locomoting cells are the sites where new membrane materials are inserted from internal pools by exocytosis (Bergmann et al., 1983; Kupfer et al., 1987; Bretscher, 1983; Ekblom et al., 1983; Bretscher and Aguado-Velasco, 1998). Previous studies directly observed exocytosis of slime-containing vesicles in *Physarum* plasmodia migrating on a solid substrate, and found that a single protrusion forms immediately after each exocytotic event in the vicinity of the site of expulsion (Sesaki and Ogihara, 1997). From quantitative measurements, they showed a linear relationship between the surface area of individual protrusions and that of the single slime-containing vesicles. In the quinine-induced protrusion in the present study, the membrane derived from the contractile vacuole constituted only a limited membrane area at the tip of the protrusion. Conceivably, insertion of contractile vacuole membrane triggers only the formation of a protrusion by providing a membrane domain with low cortical tension, while its contribution to the elongation of the protrusion is limited. The origin of the flanking part of the membrane of the protrusion remains to be clarified, but the continuous presence of both lipid and protein markers of the contractile vacuole membrane at the tip of the protrusion (Fig. 2; Fig. 3) suggests that insertion by exocytosis at the tip of the protrusion is unlikely. Presumably, lipids laterally flow from the cell body into the protruded area, as has been suggested in locomoting free-living amoebae and mammalian cells (Grębecki, 1986; Lee et al., 1990; Heath and Holifield, 1991; see Fig. 10B). The observation of conA beads being stationary to the substratum implies that their receptor proteins were anchored to the cytoskeleton and that the cytoskeleton was stationary to the substratum.

The above results indicate that the endo- and exocytosis-mediated lipid flow does not play a significant role in generating the force for the protrusion elongation. We tested other possible candidates for the source of the motive force (i.e. osmotic swelling, myosin II and actin polymerization).

In the acrosomal reaction of *Thyone* sperms, osmotic swelling of the cell has been proposed to be the main source

of the force (Tilney and Inoué, 1985; Oster and Perelson, 1987). However, quinine-induced protrusions were still capable of elongation, albeit at lower speeds, in solutions of much higher osmolarity than the cytosol. This result indicates that the force resulting from passive influx of water can only partially account for the formation of protrusions, and suggests the involvement of active processes.

Requirement of functional myosin system in bleb formation has been suggested in mammalian cells (Torgerson and McNiven, 1998; Hagmann et al., 1999). In our system, no protrusion was formed in mutant cells lacking myosin II (*mhc*$^-$ cells). In these cells, fusion of contractile vacuoles did occur (Fig. 6), indicating that their defects are not in the insertion of contractile vacuole membranes but in the generation of protrusive forces. The cortical localization of myosin II and its initial absence within the protrusions in Ax2 cells suggest that the effect of myosin II here is to cause contraction of the cell cortex, which would result in increased cortical tension and consequently a flow of the cytosol into the protrusion. This view is consistent with the significantly shorter length of cellular contents protruded out of punctured *mhc*$^-$ cells in a viscous solution, and gains further support from the reduced rate of cortical contraction (Fukui et al., 1999) and diminished cortical tension (Pasternak et al., 1989; Egelhoff et al., 1996; Dai et al., 1999) in *mhc*$^-$ cells.

Myosin II eventually accumulated in the cortex of the protrusion, progressively from its base towards the tip. When the layer of myosin II reached the distal end of the protrusion, it invariably started to retract, as in the case of natural pseudopods of *Dictyostelium* cells (Moores et al., 1996)

By contrast, our results do not support the possible role of actin polymerization in the generation of the motive force in the quinine-induced protrusions in which F-actin is either absent or scarce in the leading front. The absence of an F-actin layer in rapidly expanding protrusions have also been noted in other kinds of cells. For instance, it has been shown using cultured tumor cell lines that a newly formed bleb is devoid of a cortical layer of F-actin, but that a new cortex of F-actin forms inside the bleb soon after it has formed (Keller and Eggli, 1998; Hagmann et al., 1999). It was previously noted that the expansion rates of blebs were inversely proportional to the F-actin content in human melanoma cells, suggesting that blebs are formed when the fluid-driven expansion of the cell membrane is sufficiently rapid to outpace the local actin polymerization (Cunningham, 1995). This explanation may be applicable to our observations that F-actin was not detectable in the leading edge of rapidly elongating protrusions, whereas retracting protrusions were lined with a thick layer of F-actin all over. Also, the close correlation between the fluctuation of the elongation speed of the protrusion and the detachment of F-actin layers from its front end (Fig. 11C,D) can be best explained if the F-actin layer that is firmly attached to the membrane acts as a resistance to the expansion of the protrusion. The antagonizing effects of F-actin on the elongation of protrusions were further demonstrated by the considerably more rapid expansion of spherical blebs (as opposed to elongated directional protrusions) in cells treated with quinine plus cytochalasin A. These results suggest that the actin polymerization itself does not contribute to the protrusive force, but rather acts to restrain the protrusion from expanding sideways. However, the backward movement of the detached actin layers suggests that they were being pulled backwards by continuous contraction of the actin cortex to which they are connected. Rearward flow of cortical F-actin has been proposed to be the basis of cell movement in general

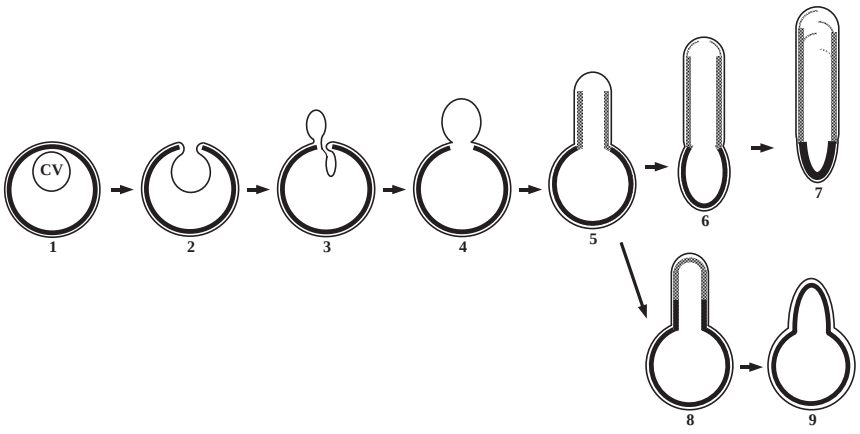

Fig. 13. A proposed model for quinine-induced protrusion formation. (1) The plasma membrane (thin line) is lined with a cortical layer of actin and myosin (thick line) which produces strong cortical tension. (2) The contractile vacuole (CV) fuses with the plasma membrane. (3) High inner pressure due to the elevated cortical tension forces the vacuolar membrane out through the hole of the cortical layer to form a protrusion. (4) Contraction of the cortical layer continues to force the cytosol into the protrusion. The protrusion expands because of the low tension of its membrane which lacks a cortical layer of F-actin. (5) A cortical layer of F-actin (grey line) extends from the cell body into the protrusion along its lateral membrane, but the absence of F-actin cortex at its distal region allows its further elongation. (6) The actomyosin layer continues to contract, pushing the cellular content forwards into the protrusion. This results in locomotion of the cell. The cortical layer of F-actin on the lateral side of the protrusion continues to elongate forwards, but the apex of the protrusion remains virtually free of F-actin or is only loosely bound to a thin actin layer (thin grey line), allowing sustained movement of the cell. (7) Forward movement of the cell continues if the actomyosin cortex at the back of the cell continues to supply forces necessary for elongation of the protrusion and if the thin actin layer continues to be detached from the membrane. Release of actin, myosin II, and other cortex-associated molecules from the cortical cytoskeleton in the tail region by a mechanism probably involving the regulation by F-actin-crosslinking proteins (Jason and Taylor, 1993) is also required for their reuse in the front. A new actin layer starts to be formed inside the apical membrane immediately after detachment of the existing actin layer, while the detached actin layer moves backwards due to contraction of the cell cortex and is gradually disintegrated (dashed grey line). The detachment of the actin layer at the tip of the protrusion may be discrete events or continuous process forming a spiral sheet of F-actin as illustrated here. (8) If the plasma membrane of the entire protrusion becomes firmly attached to the F-actin cortex, the protrusion stops extending. A layer of myosin II gradually extends from the cell body towards the leading edge. (9) The entire protrusion becomes lined with the myosin layer and the protrusion retracts.

(Bray and White, 1988) and actually demonstrated in locomoting *Dictyostelium* cells (Fukui et al., 1999).

The above considerations led us to consider the three forces that would determine the initiation and the subsequent fate of a protrusion: the cytosolic pressure, the force derived from contraction of the cortical cytoskeleton, and the force needed to detach the membrane-cytoskeleton adhesion. Whether the protrusion elongates or retracts will therefore depend on the balance between these forces. Grębecki has proposed an essentially identical model for the control of pseudopod elongation in free-living soil amoebae (Grębecki, 1990; Grębecki, 1994). Fig. 13 summarizes the model for the quinine-induced protrusion formation leading to cell locomotion or followed by its retraction.

From the viewpoint of the positional regulation of protrusive activity in general, the adhesion force between the membrane and the cortical F-actin layer will be the principal determinant as this force can be locally regulated, whereas the other two forces (cytoplasmic pressure and cortical contraction) are more globally determined. Interestingly, the leading front of protrusions often coincides with the site of exocytosis, as shown in this study and in many others (Bretscher, 1996). This raises the possibility that insertion by exocytosis of small patches of membrane that lack the molecules required for membrane-cortex adhesion might trigger and sustain protrusion extension. Rapid formation of membrane-linked F-actin layers on the lateral side of the protrusion would then prevent its uncontrolled expansion and possibly delay the diffusion of the linking molecules from the cell membrane into the leading edge. The quinine-induced protrusion might be an extreme case where a substantial area of membrane is inserted at a time.

Although actin polymerization itself has been shown to generate sufficient forces for protrusion extension and is widely believed to be a major machinery of pseudopod extension in cells firmly adhered to the substratum (reviewed by Borisy and Svitkina, 2000), the results shown in this study provide a clear example in which actin polymerization in the leading edge of a protrusion does not provide the force for its extension but rather constrain it. As mentioned above, similar situations have been described in other types of cells as diverse as locomoting free-living amoebae (Grębecki, 1990) and in Walker carcinosarcoma cells (Keller and Bebie, 1996), both exhibiting rapid locomotion by progressive extension of a large lobopodium. In fact, the antagonizing effect of F-actin on protrusion extension is not limited to blebs or lobopodia. Lamellipodial extension in mouse fibroblasts, for example, is inversely correlated with the membrane tension, which is largely determined by the membrane-associated cytoskeleton (Raucher and Sheetz, 2000). In fish keratocytes, lamellipodial extension is closely correlated with the site of low membrane tension and can be stimulated or suppressed by local application of drugs that presumably alter the stability of F-actin (and therefore membrane tension) downwards or upwards, respectively (Bereiter-Hahn and Luers, 1998). These results suggest the universality of the mechanism in which F-actin acts as a constraint on protrusion extension.

Elongation of protrusions driven by contraction of the cell cortex, as was observed in quinine-treated cells, would represent one of the native modes of pseudopod elongation, which may be called the ‘tail-contraction mode’. Protrusions of similar appearance can be found in *Dictyostelium* cells under physiological conditions. During unicellular stages of development, such protrusions can be seen only transiently before taken over by other types of protrusions, but they are very common in cells dissociated from multicellular structures (Fig. 12). In this connection, it is noteworthy that *Dictyostelium* cells lacking myosin II are only partially defective in amoeboid movement when adhered to solid substratum but their movement during multicellular morphogenesis is severely affected (Knecht and Loomis, 1987; De Lozanne and Spudich, 1987; Traynor et al., 1994; Springer et al., 1994; Knecht and Shelden, 1995; Clow and McNally, 1999). Although the ‘tail-contraction mode’ may be obscured by prominent protrusions of other modes when cells are firmly adhered to a solid substratum, it may be playing an important role in cells forming 3D multicellular structures in *Dictyostelium* and possibly in many other organisms (Trinkaus, 1973).

We thank S. Yumura, J. Spudich and D. Knecht for the strains, H. Aizawa, T. Uyeda, M. Clarke and S. Ogihara for valuable suggestions, and A. Fok and the Monoclonal Antibody Service Facility of the University of Hawaii at Manoa for providing the mAb N2.

REFERENCES

Abraham, V. C., Krishnamurthi, V., Taylor, D. L. and Lanni, F. (1999). The actin-based nanomachine at the leading edge of migrating cells. *Biophys. J.* **77**, 1721-1732.

Allen, R. D. (1961). A new theory of amoeboid movement and protoplasmic streaming. *Exp. Cell Res.* **8**, Suppl., 17-31.

Becker, M., Matzner, M. and Gerisch, G. (1999). Drainin required for membrane fusion of the contractile vacuole in *Dictyostelium* is the prototype of a protein family also represented in man. *EMBO J.* **18**, 3305-3316.

Bereiter-Hahn, J. and Luers, H. (1998). Subcellular tension fields and mechanical resistance of the lamella front related to the direction of locomotion. *Cell Biochem. Biophys.* **29**, 243-262.

Bergmann, J. E., Kupfer, A. and Singer, S. J. (1983). Membrane insertion at the leading edge of motile fibroblasts. *Proc. Natl. Acad. Sci. USA* **80**, 1367-1371.

Borisy, G. G. and Svitkina, T. M. (2000). Actin machinery: pushing the envelope. *Curr. Opin. Cell Biol.* **12**, 104-112.

Boss, J. (1955). Mitosis in cultures of newt tissues. IV. The cell surface in late anaphase and the movements of ribonucleoprotein. *Exp. Cell Res.* **8**, 181-197.

Bray, D. and White, J. G. (1988). Cortical flow in animal cells. *Science* **239**, 883-888.

Bretscher, M. S. (1983). Distribution of receptors for transferrin and low density lipoprotein on the surface of giant HeLa cells. *Proc. Natl. Acad. Sci. USA* **80**, 454-458.

Bretscher, M. S. (1984). Endocytosis: relation to capping and cell locomotion. *Science* **224**, 681-686.

Bretscher, M. S. (1996). Getting membrane flow and the cytoskeleton to cooperate in moving cells. *Cell* **87**, 601-606.

Bretscher, M. S. and Aguado-Velasco, C. (1998). EGF induces recycling membrane to form ruffles. *Curr. Biol.* **8**, 721-724.

Clow, P. A. and McNally, J. G. (1999). In vivo observations of myosin II dynamics support a role in rear retraction. *Mol. Biol. Cell* **10**, 1309-1323.

Condeelis, J. (1993). Life at the leading edge: The formation of cell protrusions. *Annu. Rev. Cell Biol.* **9**, 411-444.

Cunningham, C. C. (1995). Actin polymerization and intracellular solvent flow in cell surface blebbing. *J. Cell Biol.* **129**, 1589-1599.

Dai, J., Ting-Beall, H. P., Hochmuth, R. M., Sheetz, M. P. and Titus, M. A. (1999). Myosin I contributes to the generation of resting cortical tension. *Biophys. J.* **77**, 1168-1176.

De Lozanne, A. and Spudich, J. A. (1987). Disruption of the *Dictyostelium* myosin heavy chain gene by homologous recombination. *Science* **236**, 1086-1091.

Egelhoff, T. T., Naismith, T. V. and Brozovich, F. V. (1996). Myosin-based

cortical tension in *Dictyostelium* resolved into heavy and light chain-regulated components. *J. Muscle Res. Cell Motil.* **17**, 269-274.

Ekblom, P., Thesleff, I., Lehto, V. P. and Virtanen, I. (1983). Distribution of the transferrin receptor in normal human fibroblasts and fibrosarcoma cells. *Int. J. Cancer* **31**, 111-117.

Erickson, C. A. and Trinkaus, J. P. (1976). Microvilli and blebs as sources of reserve surface membrane during cell spreading. *Exp. Cell Res.* **99**, 375-384.

Fok, A. K., Clarke, M., Ma, L. and Allen, R. D. (1993). Vacuolar H(+)-ATPase of *Dictyostelium discoideum*. A monoclonal antibody study. *J. Cell Sci.* **106**, 1103-1113.

Fukui, Y., Kitanishi-Yumura, T. and Yumura, S. (1999). Myosin II-independent F-actin flow contributes to cell locomotion in *Dictyostelium*. *J. Cell Sci.* **112**, 877-886.

Ginger, R. S., Drury, L., Baader, C., Zhukovskaya, N. V. and Williams, J. G. (1998). A novel *Dictyostelium* cell surface protein important for both sell adhesion and cell sorting. *Development* **125**, 3343-3352.

Gręboecki, A. (1986). Two-directional pattern of movements on the cell surface of *Amoeba proteus*. *J. Cell Sci.* **83**, 23-35.

Gręboecki, A. (1990). Dynamics of the contractile system in the pseudopodial tips of normally locomoting amoebae, demonstrated in vivo by video-enhancement. *Protoplasma* **154**, 98-111.

Gręboecki, A. (1994). Membrane and cytoskelton flow in motile cells with emphasis on the contribution of free-living amoebae. *Int. Rev. Cytol.* **148**, 37-80.

Hagmann J., Burger M. M. and Dagan, D. (1999). Regulation of plasma membrane blebbing by the cytoskeleton. *J. Cell Biochem.* **73**, 488-499.

Harris, A. K. (1990). Protrusive activity of the cell surface and the movements of tissue cells. In *Biomechanics of active movement and deformation* (NATO ASI Series). Vol. H42 (ed. N. Akkas), pp. 249-291.

Heath, J. P. and Holifield, B. F. (1991). Cell locomotion: new research tests old ideas on membrane and cytoskeletal flow. *Cell Motil. Cytoskeleton* **18**, 245-257.

Heuser, J., Zhu, Q. and Clarke, M. (1993). Proton pumps populate the contractile vacuoles of *Dictyostelium* amoebae. *J. Cell Biol.* **121**, 1311-1327.

Janson, L. W. and Taylor, D. L. (1993). In vitro models of tail contraction and cytoplasmic streaming in amoeboid cells. *J. Cell Biol.* **123**, 345-356.

Jay, P. Y. and Elson, E. L. (1992). Surface particle transport mechanism independent of myosin II in *Dictyostelium*. *Nature* **356**, 438-440.

Keller, H. U. and Bebie, H. (1996). Protrusive activity quantitatively determines the rate and direction of cell locomotion. *Cell Motil. Cytoskeleton.* **33**, 241-251.

Keller, H. and Eggli, P. (1998). Protrusive activity, cytoplasmic compartmentalization, and restriction rings in locomoting blebbing Walker carcinosarcoma cells are related to detachment of cortical actin from the plasma membrane. *Cell Motil. Cytoskeleton* **41**, 181-193.

Knecht, D. A. and Loomis, W. F. (1987). Antisense RNA inactivation of myosin heavy chain gene expression in *Dictyostelium discoideum*. *Science* **236**, 1081-1086.

Knecht, D. A. and Shelden, E. (1995). Three-dimensional localization of wild-type and myosin II mutant cells during morphogenesis of *Dictyostelium*. *Dev. Biol.* **170**, 434-444.

Kupfer, A., Kronebusch, P. J., Rose, J. K and Singer, S. J. (1987). A critical role for the polarization of membrane recycling in cell motility. *Cell Motil. Cytoskeleton* **8**, 182-189.

Lee, J., Gustafsson, M., Magnusson, K.-E. and Jacobson, K. (1990). The direction of membrane lipid flow in locomoting polymorphonuclear leukocytes. *Science* **247**, 1229-1233.

Manstein, D. J., Titus, M. A., De Lozanne, A. and Spudich, J. A. (1989). Gene replacement in *Dictyostelium*: generation of myosin null mutants. *EMBO J.* **8**, 923-932.

Mast, S. (1926). Structure, movement, locomotion and stimulation in amoebae. *J. Morphol. Physiol.* **41**, 347-425.

Mogilner, A. and Oster, G. (1996). Cell motility driven by actin polymerization. *Biophys. J.* **71**, 3030-3045.

Moores, S. L., Sabry, J. H. and Spudich, J. A. (1996). Myosin dynamics in live *Dictyostelium* cells. *Proc. Natl. Acad. Sci. USA* **93**, 443-446.

Neuhaus, E. M., Horstmann, H., Almers, W., Maniak, M. and Soldati, T. (1998). Ethane-freezing/methanol-fixation of cell monolayers: a procedure for improved preservation of structure and antigenicity for light and electron microscopies. *J. Struct. Biol.* **121**, 326-342.

Nolta, K. V., Padh, H. and Steck, T. L. (1993). An immunocytochemical analysis of the vacuolar proton pump in *Dictyostelium discoideum*. *J. Cell Sci.* **105**, 849-859

Oster, G. F. and Perelson, A. S. (1987). The physics of cell motility. *J. Cell Sci. Suppl.* **8**, 35-54.

Pang, K. M., Lee, E. and Knecht, D. A. (1998). Use of a fusion protein between GFP and an actin-binding domain to visualize transient filamentous-actin structures. *Curr. Biol.* **8**, 405-408.

Pasternak, C., Spudich, J. A. and Elson, E.L. (1989). Capping of surface receptors and concomitant cortical tension are generated by conventional myosin. *Nature* **341**, 549-551.

Raucher, D. and Sheetz, M. P. (2000). Cell spreading and lamellipodial extension rate is regulated by membrane tension. *J. Cell Biol.* **148**, 127-136.

Schindl, M., Wallraff, E., Deubzer, B., Witke, W., Gerisch, G. and Sackmann, E. (1995). Cell-substrate interactions and locomotion of *Dictyostelium* wild-type and mutants defective in three cytoskeletal proteins: A study using quantitative reflection interference contrast microscopy. *Biophys. J.* **68**, 1177-1190.

Sesaki, H. and Ogihara, S. (1997). Protrusion of cell surface coupled with single exocytotic events of secretion of the slime in *Physarum* plasmodia. *J. Cell Sci.* **110**, 809-818.

Sheetz, M. P., Turney, S., Qian, H. and Elson, E. L. (1989). Nanometre-level analysis demonstrates that lipid flow does not drive membrane glycoprotein movements. *Nature* **340**, 284-288.

Springer, M. L., Patterson, B. and Spudich, J. A. (1994). Stage-specific requirement for myosin II during *Dictyostelium* development. *Development* **120**, 2651-2660.

Steck, T. L., Chiaraviglio, L. and Meredith, S. (1997). Osmotic homeostasis in *Dictyostelium discoideum*: excretion of amino acids and ingested solutes. *J. Eukaryotic Microbiol.* **44**, 503-510.

Taylor, D. L. and Condeelis, J. S. (1979). Cytoplasmic structure and contractility in amoeboid cells. *Int Rev Cytol.* **56**, 57-144.

Tilney, L. and Inoué, S. (1985). Acrosomal reaction of *Thyone* sperm. III The relationship between actin assembly and water influx during the extension of the acrosomal process. *J. Cell Biol.* **100**, 1273-1287.

Torgerson, R. R. and McNiven, M. A. (1998). The actin-myosin cytoskeleton mediates reversible agonist-induced membrane blebbing. *J. Cell Sci.* **111**, 2911-2922

Traynor, D., Tasaka, M., Takeuchi, I. and Williams, J. (1994). Aberrant pattern formation in myosin heavy chain mutants of *Dictyostelium*. *Development* **120**, 591-601.

Trinkaus, J. P. (1973). Surface activity and locomotion of *Fundulus* deep cells during blastura and gastrula stages. *Dev. Biol.* **30**, 68-103.

Van Duijn, B., Van der Molen, L. G. and Ypey, D. L. (1989). Effects of potassium channel blockers on differentiation of *Dictyostelium discoideum*. *Pflugers Archiv.* **414**, Suppl 1, S148-S149.

Wang, Y. L. (1985). Exchange of actin subunits at the leading edge of living fibroblasts: possible role of treadmilling. *J. Cell Biol.* **101**, 597-602.

Watts, D. J. and Ashworth, J. M. (1970). Growth of myxameobae of the cellular slime mould *Dictyostelium discoideum* in axenic culture. *Biochem. J.* **119**, 171-174.

Yanai, M., Kenyon, C. M., Butler, J. P., Macklem, P. T. and Kelly, S. M. (1996). Intracellular pressure is a motive force for cell motion in *Amoeba proteus*. *Cell Motil. Cytoskeleton* **33**, 22-29.

Yoshida, K., Ide, T., Inouye, K., Mizuno, K., Taguchi, T. and Kasai, M. (1997). A voltage- and K^+-dependent K^+ channel from a membrane fraction enriched in contractile vacuole of *Dictyostelium discoideum*. *Biochim. Biophys. Acta* **1325**, 178-188.

Zhu, Q. and Clarke, M. (1992). Association of calmodulin and an unconventional myosin with the contractile vacuole complex of *Dictyostelium discoideum*. *J. Cell Biol.* **118**, 347-358.